Novel Mechanistic Class of Fatty Acid Amide Hydrolase Inhibitors with Remarkable Selectivity[†]

Kyunghye Ahn,*,[‡] Douglas S. Johnson,[‡] Laura R. Fitzgerald,[‡] Marya Liimatta,[‡] Andrea Arendse,[‡] Tracy Stevenson,[‡] Eric. T. Lund,[‡] Richard A. Nugent,[§] Tyzoon K. Nomanbhoy,[||] Jessica P. Alexander,[⊥] and Benjamin F. Cravatt[⊥]

Pfizer Global Research and Development, Ann Arbor, Michigan 48105, Pfizer Global Research and Development, Cambridge, Massachusetts 02139, ActivX Biosciences, 11025 North Torrey Pines Road, La Jolla, California 92037, and Departments of Chemical Physiology, The Skaggs Institute for Chemical Biology, The Scripps Research Institute, 10550 North Torrey Pines Road, La Jolla, California 92037

ABSTRACT: Fatty acid amide hydrolase (FAAH) is an integral membrane enzyme that degrades the fatty acid amide family of signaling lipids, including the endocannabinoid anandamide. Genetic or pharmacological inactivation of FAAH leads to analgesic, anti-inflammatory, anxiolytic, and antidepressant phenotypes in rodents without showing the undesirable side effects observed with direct cannabinoid receptor agonists, indicating that FAAH may represent an attractive therapeutic target for treatment of pain, inflammation, and other central nervous system disorders. However, the FAAH inhibitors reported to date lack drug-like pharmacokinetic properties and/or selectivity. Herein we describe piperidine/piperazine ureas represented by *N*-phenyl-4-(quinolin-3-ylmethyl)piperidine-1-carboxamide (PF-750) and *N*-phenyl-4-(quinolin-2-ylmethyl)piperazine-1-carboxamide (PF-622) as a novel mechanistic class of FAAH inhibitors. PF-750 and PF-622 show higher in vitro potencies than previously established classes of FAAH inhibitors. Rather unexpectedly based on the high chemical stability of the urea functional group, PF-750 and PF-622 were found to inhibit FAAH in a time-dependent manner by covalently modifying the enzyme's active site serine nucleophile. Activity-based proteomic profiling revealed that PF-750 and PF-622 were completely selective for FAAH relative to other mammalian serine hydrolases. We hypothesize that this remarkable specificity derives, at least in part, from FAAH's special ability to function as a C(O)−N bond hydrolase, which distinguishes it from the vast majority of metabolic serine hydrolases in mammals that are restricted to hydrolyzing esters and/or thioesters. The piperidine/piperazine urea may thus represent a privileged chemical scaffold for the synthesis of FAAH inhibitors that display an unprecedented combination of potency and selectivity for use as potential analgesic and anxiolytic/antidepressant agents.

Fatty acid amide hydrolase (FAAH[1]) is an integral membrane enzyme (*1, 2*) that regulates the fatty acid amide family of lipid transmitters, which includes the endogenous cannabinoid *N*-arachidonyl ethanolamine (anandamide) (*3*), the anti-inflammatory factor *N*-palmitoyl ethanolamine (PEA) (*4*), the sleep-inducing substance 9(*Z*)-octadecenamide (oleamide) (*5*), and the satiating signal *N*-oleoyl ethanolamine (OEA) (*6*).

FAAH inactivation by either genetic deletion of the *FAAH* gene in mice (*7*) or by chemical inhibitors (*8*) leads to elevated endogenous levels of fatty acid amides with concomitant analgesic (*9−13*), anxiolytic (*8*), antidepressant (*14, 15*), sleep-enhancing (*16*), and anti-inflammatory (*9, 17, 18*) phenotypes. Notably the behavioral phenotypes observed in FAAH knockout (−/−) mice (*7, 9*) or in rodents treated with FAAH inhibitors (*8, 11−14, 18*) occur in the absence of alterations in motility, weight gain, or body temperature that are typically observed with direct cannabinoid receptor 1 (CB1) agonists. These findings suggest that FAAH may represent an attractive therapeutic target for treatment of pain, inflammation, and other central nervous system (CNS) disorders and has stimulated interest in the development of selective inhibitors of this enzyme.

FAAH is a member of an unusual class of serine hydrolases termed the amidase signature family (*19*) that utilizes a serine−serine−lysine catalytic triad. The mechanistic features of FAAH have been described in a recent review (*20*). Despite its unique catalytic mechanism, FAAH can be inhibited by several classical types of serine hydrolase inhibitors including fluorophosphonates (*21*), trifluoromethyl ketones (*22*), α-keto heterocycles (*23, 24*), and carbamates (*8*), which have all been shown to exhibit high in vitro potencies. Carbamate inhibitors, best exemplified by URB-

* To whom correspondence should be addressed: Phone: (860) 686-9406. Fax: (860) 715-4608. E-mail: kay.ahn@pfizer.com.

[‡] Pfizer Global Research and Development, Ann Arbor, Michigan.

[§] Pfizer Global Research and Development, Cambridge, Massachusetts.

[||] ActivX Biosciences.

[⊥] The Scripps Research Institute.

[1] Abbreviations: ABPP, activity-based protein profiling; CNS, central nervous system; EDTA, ethylenediaminetetraacetic acid; FAAH, fatty acid amide hydrolase; FP, fluorophosphonate; FP-Rh, fluorophosphonate carboxytetramethylrhodamine; GDH, glutamate dehydrogenase; HEPES, 4-(2-hydroxyethyl)-1-piperazineethanesulfonic acid; i.p., intraperitoneal; MS, mass spectrometry; NADH, nicotinamide adenine dinucleotide (reduced form); NAD^{+}, nicotinamide adenine dinucleotide (oxidized form); SDS-PAGE, sodium dodecyl sulfate-polyacrylamide gel electrophoresis; TFA, trifluoroacetic acid.
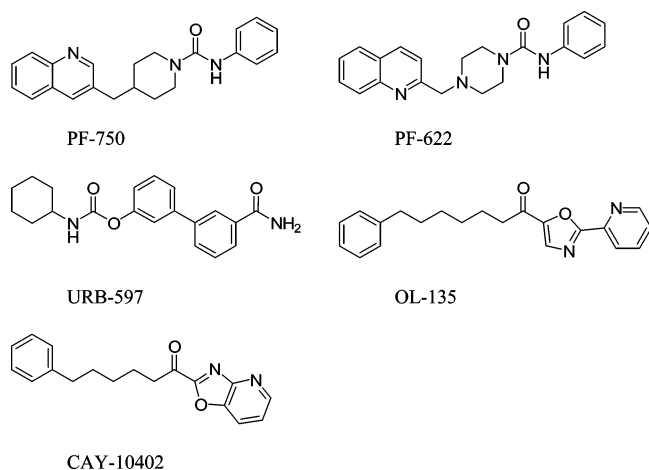
FIGURE 1: Structures of various FAAH inhibitors.

597 (*8*), are particularly efficacious in vivo, displaying activity in rodent models of inflammatory (*12*, *18*) and neuropathic pain (*13*) as well as anxiety and depression (*8*, *14*, *15*). However, each of the aforementioned classes of FAAH inhibitors lacks drug-like pharmacokinetic properties and/or selectivity (*25*−*28*). During our search for novel FAAH inhibitors, we conducted a high-throughput screen of the Pfizer chemical library and identified a new chemical series of agents that share a piperidine/piperazine urea scaffold. Improvements made to potency and drug-like properties engendered the FAAH inhibitors *N*-phenyl-4-(quinolin-3-ylmethyl)piperidine-1-carboxamide (PF-750) and *N*-phenyl-4-(quinolin-2-ylmethyl)piperazine-1-carboxamide (PF-622) shown in Figure 1. Here, we report a detailed characterization of the mechanism of inhibition and selectivity of PF-750 and PF-622 using enzyme kinetic and functional proteomic methods. We provide direct evidence that PF-750 and PF-622, despite their high chemical stability, covalently inactivate FAAH via carbamylation of the enzyme's catalytic serine nucleophile. PF-750 and PF-622 did not show any detectable activity against other serine hydrolases in mammalian proteomes. Our findings thus promote piperidine/piperazine ureas as a privileged molecular scaffold for creating covalent inhibitors of FAAH that display an unprecedented combination of potency and selectivity.

MATERIALS AND METHODS

Materials. Oleamide was purchased from Sigma. Nicotinamide adenine dinucleotide, reduced form (NADH), and glutamate dehydrogenase (GDH) were from Roche Diagnostics. Triton X-100 and ethylenediaminetetraacetic acid (EDTA) were obtained from Calbiochem and Biochemika, respectively. ADP and α-ketoglutaric acid were purchased from Amresco. URB-597 and CAY-10402 were purchased from Cayman Chemicals (Ann Arbor, MI). Inhibitors were stored as dry powders at RT (−20 °C for URB-597) and dissolved in DMSO to prepare concentrated stock solutions on the day of the experiments. Polystyrene 96-well microplates were purchased from Rainin. All reagents used were the highest quality commercially available. Mouse and human proteomes were purchased from Pelfreeze (Rogers, AZ) and Analytical Biological Services (Wilmington, DE), respectively. Synthesis of a rhodamine-tagged fluorophosphonate (fluorophosphonate carboxytetramethylrhodamine, FP-Rh) has previously been described (*29*).

Inhibitor Synthesis. OL-135 was synthesized according to the published procedure (*24*). *N*-Phenyl-4-(quinolin-2-ylmethyl)piperazine-1-carboxamide (PF-622) was synthesized from the reductive amination of 2-quinoline-carboxaldehyde with *N*-phenylpiperazine-1-carboxamide similar to that described in the patent literature (*30*). MS(APCI) M + 1 = 347.15; ^{1}H NMR (400 MHz, DMSO-d_6) δ ppm 2.43−2.47 (m, 4 H + DMSO) 3.44 (t, J = 4.68 Hz, 4 H) 3.78 (s, 2 H) 6.88 (t, J = 7.41 Hz, 1 H) 7.18 (t, J = 7.80 Hz, 2 H) 7.40 (d, J = 7.60 Hz, 2 H) 7.55 (t, J = 7.02 Hz, 1 H) 7.64 (d, J = 8.38 Hz, 1 H) 7.69 (t, J = 7.40 Hz, 1 H) 7.92 (t, J = 7.02 Hz, 2 H) 8.31 (d, J = 8.39 Hz, 1 H), and 8.48 (s, 1H). [3H]-PF-622A was prepared by treating PF-622 with 1.1 Ci carrier-free tritium gas in the presence of Crabtree's catalyst (Ir[(COD)(PCy$_3$)(Py)]PF$_6$) in CH$_2$Cl$_2$. [3H]PF-622B was prepared by reducing *N*-(4-bromophenyl)-4-(quinolin-2-yl-methyl)piperazine-1-carboxamide with 1.1 Ci carrier-free tritium gas in the presence of Pd(PPh$_3$)$_4$ in DMF. The details of these selective tritiations will be described in a separate publication.

Synthesis of N-Phenyl-4-(quinolin-3-ylmethyl)piperidine-1-carboxamide (PF-750). (Methyl)triphenylphosphonium bromide (2.69 g, 7.52 mmol) was suspended in THF (15 mL) at 0 °C and then treated with *n*-BuLi (2 M in cyclohexane, 3.64 mL, 7.28 mmol) to generate a yellow suspension. After stirring for 45 min, *tert*-butyl 4-oxopiperidine-1-carboxylate (1.00 g, 5.02 mmol) in THF (3 mL) was added slowly. After 15 h, the reaction was quenched with H$_2$O and extracted with heptane (three times). The solution was dried over magnesium sulfate and then filtered through a pad of SiO$_2$, which was washed with heptane. The filtrates were concentrated to provide *tert*-butyl 4-methylenepiperidine-1-carboxylate (637 mg, 3.23 mmol, 64%). The colorless oil was used without further purification.

tert-Butyl 4-methylenepiperidine-1-carboxylate (19.75 g, 100.1 mmol) in THF (40 mL, previously degassed by bubbling with nitrogen for 30 min) was treated with 9-BBN (0.5 M in THF, 200 mL, 100 mmol) and heated to reflux for 1 h. After cooling, the reaction mixture was treated with 3-bromoquinoline (22.91 g, 110 mmol) and Pd(PPh$_3$)$_4$ (1.735 g, 1.502 mmol). After 15 min, potassium carbonate (20.8 g, 150 mmol) was added and the mixture was heated to reflux. After 3 h, additional THF was added (50 mL) and the reaction mixture was heated an additional 1 h. The reaction mixture was cooled and stirred an additional 16 h. After partitioning between ethyl acetate and 10% aq NaOH the organic layer was separated and the aqueous layer extracted again with EtOAc. The combined organic layers were dried over sodium sulfate, filtered, and concentrated. The crude material was purified by flash chromatography on silica (80:20 hexanes:EtOAc to 60:40 hexanes:EtOAc) to afford 13.6 g (42%) of *tert*-butyl 4-(quinolin-3-ylmethyl)piperidine-1-carboxylate. ^{1}H NMR (400 MHz, DMSO-d_6) δ ppm 1.06 (qd, J = 12.28, 4.29 Hz, 2 H) 1.35 (s, 9 H) 1.55 (d, J = 12.48 Hz, 2 H) 1.70−1.85 (m, 1 H) 2.70 (d, J = 7.21 Hz, 2 H) 3.89 (d, J = 12.67 Hz, 2 H) 7.56 (ddd, J = 8.09, 6.92, 1.36 Hz, 1 H) 7.67 (ddd, J = 8.43, 6.87, 1.46 Hz, 1 H) 7.89 (dd, J = 8.09, 1.27 Hz, 1 H) 7.96 (d, J = 8.38 Hz, 1 H) 8.10 (d, J = 1.95 Hz, 1 H) 8.74 (d, J = 2.14 Hz, 1 H).

tert-Butyl 4-(quinolin-3-ylmethyl)piperidine-1-carboxylate (13.2 g, 40.4 mmol) in dichloromethane (60 mL) was treated with trifluoroacetic acid (30 mL) and stirred at ambient

temperature for 2 h. Toluene was added, and the reaction mixture was concentrated. The residue was partitioned between dichloromethane and saturated aqueous sodium carbonate. The organic layer was washed again with saturated aqueous sodium carbonate, dried over sodium sulfate, filtered, and concentrated to give the deprotected piperidine (9.6 g). All of the deprotected material was dissolved in dichloromethane:toluene (1:1, 50 mL) and treated with phenylisocyanate (1.85 g, 15.6 mmol) followed by triethylamine (0.49 mL, 3.54 mmol). The reaction mixture was stirred 72 h and treated with saturated aqueous sodium bicarbonate. The mixture was partitioned between ethyl acetate and water. The organic layer was separated, dried over sodium sulfate, filtered, and concentrated. Flash chromatography on silica (dichloromethane to 95:5 dichloromethane:EtOH containing 11% saturated aqueous ammonium hydroxide) afforded 2.35 g of *N*-phenyl-4-(quinolin-3-ylmethyl)piperidine-1-carboxamide (PF-750) as a white solid. A significant amount of mixed fractions was rechromatographed to afford an additional 0.965 g of PF-750, resulting in a total yield of 3.315 g (68%). MS(APCI) M + 1 = 346.3; ^{1}H NMR (400 MHz, chloroform-*d*) δ ppm 1.31 (ddd, J = 12.64, 12.37, 4.20 Hz, 2 H) 1.73 (d, J = 12.69 Hz, 2 H) 1.78−1.92 (m, 1 H) 2.75 (d, J = 7.22 Hz, 2 H) 2.81 (td, J = 12.88, 2.73 Hz, 2 H) 4.07 (dt, J = 13.42, 2.07 Hz, 2 H) 6.44 (s, 1 H) 6.96−7.04 (m, 1 H) 7.22−7.29 (m, 2 H) 7.30−7.36 (m, 2 H) 7.54 (ddd, J = 8.10, 6.93, 1.17 Hz, 1 H) 7.67 (ddd, J = 8.39, 6.93, 1.46 Hz, 1 H) 7.77 (dd, J = 8.10, 1.27 Hz, 1 H) 7.89 (d, J = 1.95 Hz, 1 H) 8.09 (d, J = 8.20 Hz, 1 H) 8.75 (d, J = 2.15 Hz, 1 H).

Human FAAH (hFAAH). Recombinant truncated hFAAH encoding amino acid residues 32−579 was expressed in *E. coli* strain BL21-AI (Invitrogen) as NH$_2$-terminal His$_6$-tag fusion protein. The NH$_2$-terminal amino acid residues 1−31 constitute a predicted transmembrane domain, and this deletion greatly enhanced expression and purification similar to those shown for rat FAAH (*31*). Further details of hFAAH expression and purification procedures will be described elsewhere. Purified hFAAH used in the present study had a greater than 95% purity based on SDS-PAGE visualized by Coomassie Blue staining. Protein concentration was determined using the BCA protein assay kit (Pierce, Rockford, IL) with bovine albumin serum as standards.

FAAH Assay. FAAH activity was measured by following the production of ammonia generated from the hydrolysis of oleamide by FAAH. GDH catalyzes the condensation of ammonia and α-ketoglutarate to glutamate with a concomitant conversion of NADH to nicotinamide adenine dinucleotide, oxidized form (NAD$^+$), which is spectrophotometrically measured at 340 nm as described (*32, 33*). The assay mixture (200 μL) contained 50 mM NaPi, pH 7.4, 50 μM oleamide, 150 μM NADH, 3 mM α-ketoglutarate, 2 mM ADP, 1 mM EDTA, 7.5 unit/mL GDH, 0.1% Triton X-100, and the indicated amounts of hFAAH.

Determination of IC$_{50}$ Values. The reactions were carried out in 96-well clear polystyrene plates in a total volume of 200 μL. To a reaction mixture (140 μL) containing NaPi, pH 7.4, NADH, α-ketoglutarate, ADP, EDTA, and GDH to final concentrations of 50 mM, 150 μM, 3 mM, 2 mM, 1 mM, and 7.5 unit/mL, respectively, was added 20 μL of compounds dissolved in 50% DMSO (20 μL of 50% DMSO for controls). After the resulting mixture was mixed in a plate

Table 1: IC$_{50}$ Values of FAAH Inhibitors with Various Preincubation Times[a]

preincubation time (min)	IC$_{50}$ (μM)			
	OL-135	URB-597	PF-750	PF-622
5	0.297	0.986	0.595	0.991
15	0.208	0.856	0.248	0.687
30	0.252	0.572	0.0519	0.473
60	0.230	0.109	0.0162	0.0330

[a] Initial rates were determined using a microplate reader as described under Materials and Methods. The concentrations of inhibitors were varied from 0.0048 to 10 μM. IC$_{50}$ values were determined as described in the Figure 2 legend.

vortex, 20 μL of hFAAH (370 ng) in 20 mM NaPi, pH 7.8/1% Triton X-100, was added and mixed. After this mixture was preincubated at RT for the indicated period of time the reaction was initiated by addition of 20 μL of 500 μM oleamide dissolved in 25% DMSO and 75% EtOH. The final concentrations of DMSO and EtOH were each 7.5%, which have no effect on FAAH and GDH activities (data not shown). The reactions were incubated at 30 °C, and the absorbance at 340 nm was collected over a period of 30 min with readings taken in 10-s intervals using a SpectraMax Microplate Spectrophotometer (Molecular Devices, Palo Alto, CA) equipped with Softmax Pro software (Molecular Devices, Palo Alto, CA). A background rate determined for samples containing no hFAAH was subtracted from all reactions to calculate the initial rates. Initial rates were plotted as percentage of inhibition relative to uninhibited control reactions versus inhibitor concentration.

Reversibility Studies. The reversibility of hFAAH inactivation by inhibitors was assessed by rapid dilution. In a total volume of 50 μL, human FAAH (5.3 μg) was incubated at RT for 1 h with inhibitors (or DMSO for controls) at concentrations of approximately 20-fold greater than their IC$_{50}$ values with 5 min preincubation (Table 1). Immediately after an aliquot (5 μL) of the enzyme−inhibitor mixture was diluted 300-fold into the FAAH assay mixture, 200 μL of the diluted reaction mixture was placed in the wells of the microplates. The reaction mixture was incubated at 30 °C, and absorbance changes were measured over a period of 50 min using a microplate reader as described under FAAH Assay.

Incorporation of [^{3}H]PF-622 into hFAAH. Reaction mixtures contained 50 mM NaPi, pH 7.4, 50 mM NaCl, 0.1% Triton X-100, 10 μM [^{3}H]PF-622 (7700 Ci/mol), and 1.6 μg of hFAAH. For background (nonspecific binding), hFAAH was denatured by heating at 85 °C for 10 min before addition of [^{3}H]PF-622. After incubating the mixtures for 5 h at RT, 400 μL of cold acetone was added, and the final mixture was placed on ice for 20 min and kept at −80 °C overnight. The mixtures were centrifuged at 10 000*g* at 4 °C for 30 min, and the resulting pellets were washed three times with 1.5 mL of ice-cold acetone and allowed to dry at RT for 2 h. The pellets were resuspended in the SDS-PAGE loading buffer, heated at 70 °C for 10 min, and subjected to SDS-PAGE (10% Bis-Tris gel with SDS-MOPS running buffer, Novex). Gels were fixed for 30 min in 25% methanol and 10% acetic acid, soaked in Amplify Fluorographic Reagent (Amersham) for 30 min, and vacuum dried. Dried gels were exposed for approximately 65 h at −80 °C to

hyperfilm-MP preflashed with Sensitize (Amersham) using a Transcreen LE intensifying screen (Kodak). For quantitative analysis, the above pellets were resuspended in 20 μL of 2% SDS, incubated at 70 °C for 10 min, and transferred to vials for counting. MicroScint-20 scintillation fluid (1 mL, Perkin-Elmer) was added to the vials, which were counted for 2 min.

Mass Spectrometry (MS) Analysis of Covalent Labeling Site of hFAAH by PF-750 and PF-622. Reaction mixtures in a final volume of 75 μL contained 10 mM Hepes, pH 7.4, 0.1% Triton X-100, 12 μg hFAAH, and 10 μM PF-622 or PF-750 (or DMSO for controls). The final concentration of DMSO was kept at 1%. After incubating the mixtures at RT for 6 h, the 5× SDS-PAGE sample buffer was added to 20 μL aliquots, and the resulting samples were subjected to SDS-PAGE. After visualizing FAAH bands by Coomassie Blue staining, the bands were excised, reduced with DTT, alkylated with iodoacetic acid, and digested with trypsin at 37 °C overnight according to established procedures (*34*). The tryptic peptides were extracted from the excised gel bands by 5% formic acid (20 μL) and desalted by C18ZipTip (Millipore). The final 2 μL elution by 50% (v/v) acetonitrile/water with 1% trifluoroacetic acid (TFA) was analyzed by MALDI-TOF MS and MS/MS on the 4700 TOF/TOF Proteomic Analyzer (Framingham, MA) with 1:2 α-cyano-4-hydroxycinnamic acid:sample (1 μL total volume spotted). MS data were searched against the Swiss-Prot and NCBI non-redundant protein databases using the Mascot search engine software (*35*).

In Vitro Proteome Selectivity Profiling. Tissues were processed to isolate membrane and soluble proteomes as previously described (*36*). Briefly, mouse and human tissues were Dounce-homogenized in the lysis buffer containing 20 mM HEPES, pH 7.5, and 20% sucrose followed by a low-speed spin (1400g, 3 min) to remove debris. The supernatant was then subjected to centrifugation at 145 000g for 45 min to provide the soluble fraction in the supernatant and the membrane fraction as a pellet that was washed and resuspended in the lysis buffer by sonication. Total protein concentration in each fraction was determined using a protein assay kit (Bio-Rad, Hercules, CA). Samples were stored at −80 °C until use.

Inhibitor selectivity was examined using competitive activity-based protein profiling (ABPP) as described previously (*37*). Briefly, soluble and membrane proteomes (5 mg/mL) were incubated at RT for 1 h with either inhibitors (PF-750 at 500 μM; URB-597, OL-135, and CAY-10402 at 100 μM) or DMSO in a final volume of 18 μL. This was followed by overnight incubation (typically 18 h) at 4 °C. Proteomes were then labeled with 5 μM FP-Rh for 20 min in a final volume of 20 μL. The reactions were quenched with an equal volume of 2× SDS-PAGE loading buffer, loaded into 96-well 10.5% SDS-PAGE gels, and subjected to electrophoresis for 105 min at 600 V. All liquid handling steps including gel loading were carried out robotically on the Tecan Genesis Freedom 200 (Männedorf, Switzerland). After electrophoresis the gels were scanned on an FMBio II flatbed fluorescence scanner (MiraiBio, San Francisco, CA) using a 605 nm band pass filter for detecting rhodamine fluorescence. The scanned gel images were analyzed with a lane-finding algorithm, resulting in generation of lane traces of the rhodamine-labeled proteins for each of the 96 lanes of the gel (molecular weight versus fluorescence intensity). The details of this lane-finding algorithm will be published elsewhere. For each proteome, lane traces of samples containing inhibitor were compared to DMSO control lanes. Gel bands in the inhibitor-treated samples whose fluorescence decreased by more than 50% relative to the corresponding gel band in the control sample were considered inhibited.

MS of Probe-Labeled Peptides. Preparation of samples for mass spectrometry has been previously described (*38*): Briefly, duplicate samples were incubated with inhibitors (or DMSO for controls) and then labeled with FP-Rh as described above (*29*). Samples were denatured with urea, reduced with DTT, alkylated with iodoacetamide, and gel-filtered in 10 mL of Econo-Pac 10DG columns (BioRad) to remove excess reagents and exchange the buffer. The gel-filtered samples were digested with trypsin, and the probe-labeled peptides were captured with rhodamine antibodies. The captured peptides were eluted by 50% CH_3CN/water with 0.1% TFA.

Samples were analyzed by LC-MS/MS on LCQ Deca XP ion trap mass spectrometers (Thermo Finnigan, San Jose, CA) as described previously (*38*, *39*). Data were searched using the Sequest algorithm (*40*) against the UniRef100 database with searching and scoring modifications described previously (*38*, *39*). An automated program generated at ActivX was used to identify inhibited peptides by comparing the intensities of parent ion peptides in samples containing inhibitor to control samples (*39*). Approximate IC_{50} values were determined for the inhibited peptides by plotting the percentage inhibition versus the inhibitor concentration and fitting the points to the Hill equation.

In Vivo Proteome Selectivity Profiling. A mix of male and female C57BL/6 mice with weights between 18 and 25 g and ages between 6 and 15 weeks were used. Mice were given intraperitoneal (i.p.) injections of 0, 10, or 30 mg/kg URB597 or 0, 10, or 30 mg/kg PF-750 (in vehicle 18:1:1 saline:emulphor:EtOH). The 0 mg/kg injections consisted solely of vehicle. One male mouse was used for each 30 mg/kg injection as well as one vehicle control. After 1 h, the mice were sacrificed by CO_2 asphyxiation and relevant tissues were flash frozen (liquid N_2) immediately upon removal. Tissues were processed to isolate membrane and cytosolic proteomes as described in In Vitro Proteome Selectivity Profiling, except that 10 mM sodium/potassium phosphate buffer (pH 8) (PB) was used as the lysis buffer instead.

Soluble and membrane proteomes of mouse tissues were diluted to 1 mg/mL in PB buffer and reacted with a rhodamine-tagged fluorophosphonate ABPP probe (FP-Rh) (*29*) at a final concentration of 1 μM in a total reaction volume of 50 μL. Reactions were quenched after 1 h with one volume 2× SDS loading buffer (reducing with protease inhibitor), run on SDS-PAGE, and visualized using an Hitachi FMBio IIe flatbed laser-induced fluorescence scanner (MiraiBio, Alameda, CA), as described previously (*27*, *37*)

RESULTS

Inhibition of hFAAH by PF-750 and PF-622 is Time Dependent. As an initial step to characterize the mechanism of action of the urea inhibitors PF-750 and PF-622, their IC_{50} values were measured following variable preincubation
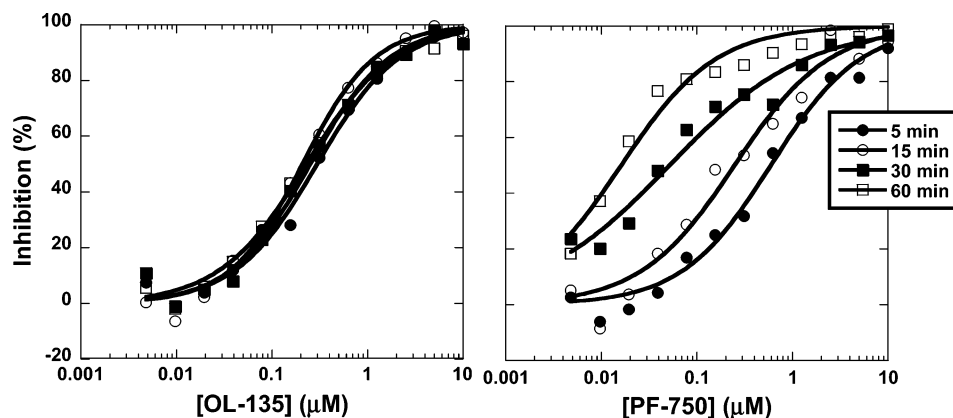
FIGURE 2: FAAH inhibition by PF-622 and PF-750 is time-dependent. Initial rates were determined using a microplate reader as described under Materials and Methods. The concentrations of OL-135 and PF-750 were varied from 0.048 to 10 μM. Three separate experiments were performed with similar results, and one experiment has been represented. The data were plotted as percentage of inhibition versus inhibitor concentration and fit to the equation, $y = 100/1 + (x/IC_{50})^z$, using KaleidaGraph (Synergy Software, Reading, PA), where IC_{50} is the inhibitor concentration at 50% inhibition and z is the Hill slope (the slope of the curve at its inflection point).

times. hFAAH was preincubated with inhibitors for 5, 15, 30, and 60 min before initiating the reaction by addition of the FAAH substrate oleamide. OL-135 and URB-597, known reversible and irreversible inhibitors of FAAH, respectively, were also included in this experiment for comparison. PF-750 exhibited a dramatic elevation in potency as the preincubation time increased (Figure 2); PF-750 inhibited hFAAH approximately 2.4-, 11-, and 37-fold more potently with 15-, 30-, and 60-min preincubation time, respectively, compared to its potency with a 5-min preincubation time (Table 1). A similar time-dependent inhibition was observed for PF-622 (Table 1). URB-597 also showed a time-dependent inhibition with a lower potency increase of 9.0-fold over the preincubation time course (Table 1). In contrast, OL-135 did not change its potency regardless of the preincubation time (Figure 2 and Table 1).

Reversibility Studies of the Urea Inhibitors (Rapid Dilution). To assess whether PF-750 and PF-622 acted as reversible or irreversible inhibitors, a rapid dilution experiment was carried out. hFAAH was incubated with inhibitors (or DMSO as a control) at concentrations approximately 20-fold higher than their IC_{50} values obtained with 5-min preincubation; under these conditions, hFAAH is expected to be completely inhibited. After incubation for 1 h at RT, the mixture was rapidly diluted 300-fold with buffer containing substrate oleamide and the recovery of FAAH activity was measured. In this assay, inhibition by OL-135 was rapidly reversible and the recovered activity was indistinguishable from the control reaction preincubated with DMSO (Figure 3). In contrast, enzyme preincubated with PF-750 and PF-622 did not recover activity. Even after 50 min, FAAH activity was similar to that observed in completely inhibited samples. A similar negligible recovery of FAAH activity was also observed with URB-597, a known irreversible inhibitor (*27*) (Figure 3). These data combined with the time-dependent inhibition shown above for PF-750 and PF-622 indicated two possible modes of inhibition: (i) slowly reversible time-dependent inhibition which involves a tightening of EI to form EI* (Scheme 1) or (ii) covalent irreversible inhibition (Scheme 1 where k_4 is zero).

Determination of Covalent Bond Formation between Urea Inhibitors and hFAAH. In order to clarify the inhibition mode of PF-750 and PF-622, we next carried out experiments to
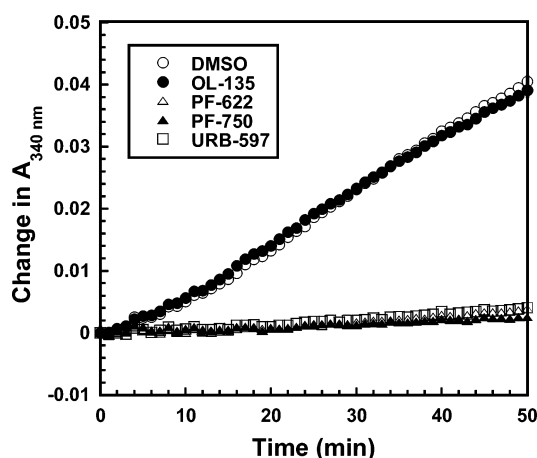

FIGURE 3: Reversibility of FAAH inactivation by FAAH inhibitors. hFAAH was incubated with FAAH inhibitors (or DMSO for controls) at concentrations of approximately 20-fold greater than their IC_{50} values with a 5 min preincubation time shown in Table 1. Aliquots of the enzyme−inhibitor mixture were diluted 300-fold into the FAAH assay mixture as described under FAAH assay in Materials and Methods, and 200 μL of the diluted reaction mixture was placed in the wells of the microplates. The reversibility of FAAH inactivation by PF-750 (▲), PF-622 (△), URB-597 (□), and OL-135 (●) was assessed by incubating the mixture at 30 °C, and absorbance changes were measured over a period of 50 min. DMSO controls are also shown (○) ($n = 4$).

Scheme 1

$$E \;+\; I \;\underset{k_2}{\overset{k_1[I]}{\rightleftharpoons}}\; EI \;\overset{k_3}{\underset{k_4}{\dashrightarrow}}\; EI^*$$
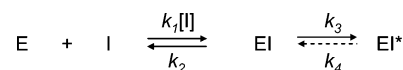
directly test whether PF-750 and PF-622 covalently modified hFAAH. Examining the structures of PF-750 and PF-622 for their potential covalent irreversible inhibition, there are two possible leaving groups generated from nucleophilic attack by the Ser241 residue as shown in Scheme 2. In order to differentiate the distinct carbamylation adducts with Ser241, we prepared PF-622 with tritium labeling in two different places. In [³H]PF-622A the tritium was incorporated into the piperazine ring, and in [³H]PF-622B the tritium was incorporated into the aniline moiety (Figure 4A). [³H]PF-622A and [³H]PF-622B were then incubated with hFAAH, and excess unincorporated inhibitor was eliminated by removing the supernatant following cold acetone precipita-

Scheme 2
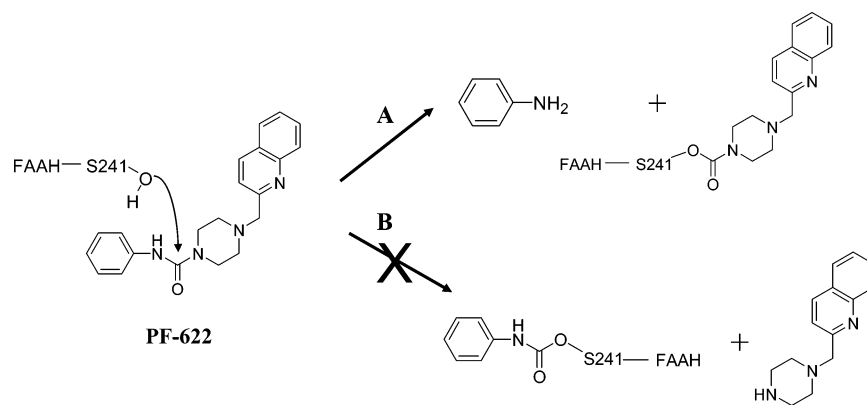
PF-622

tion. hFAAH in the precipitates was then resuspended by heating in SDS-PAGE loading buffer. To determine non-specific binding of [^{3}H]PF-622A/B to hFAAH, hFAAH was first denatured by heating at 85 °C for 10 min and then incubated with [^{3}H]PF-622A/B. Aliquots from each sample were subjected to scintillation counting, SDS-PAGE analysis, and autoradiography. As shown in Figure 4B, autoradiography identified a radioactive FAAH band at ~62 kDa with [^{3}H]PF-622A but not [^{3}H]PF-622B, indicating that the piperazine-containing moiety of PF-622 was covalently incorporated into hFAAH by pathway A in Scheme 2. By scintillation counting, samples treated with [^{3}H]PF-622A showed a signal of 48 000 dpm, which was much higher than signals observed in samples treated with [^{3}H]PF-622B or denatured FAAH samples (~5000 dpm each).

In order to determine the fragment of urea inhibitors covalently attached to hFAAH, purified recombinant enzyme was treated with PF-750 or PF-622 for 1 h and then subjected

A.

FIGURE 4: Incorporation of [^{3}H]PF-622 into hFAAH. (A, upper panel) Structures of [^{3}H]PF-622A/B. (A, lower panel) hFAAH was incubated with 10 μM [^{3}H]PF-622A/B, and excess unincorporated inhibitor was eliminated by removing supernatant following cold acetone precipitation. hFAAH from the precipitate was resuspended by heating in the SDS-PAGE loading buffer, and aliquots from each sample were counted in the scintillation counter (black bars). To measure nonspecific binding, hFAAH was first denatured by heating and then incubated with 10 μM [^{3}H]PF-622A/B (hatched bars) as described in Materials and Methods. (B) Aliquots from above were also subjected to SDS-PAGE and autoradiography.

to tryptic digestion, SDS-PAGE, and MALDI-TOF MS analysis. In both cases, new mass signals were observed with the inhibitor-treated samples compared to DMSO-treated controls. The inhibitor-modified peptides corresponded to masses of the tryptic peptide containing the Ser241 nucleophile (amino acids 213−243) adducted to the C(O)-piperazinyl moiety of PF-622 (calculated MH$^+$ = 2924. 46, observed MH$^+$ = 2924.53) (Figure 5B) and PF-750 (calculated MH$^+$ = 2923. 47, observed MH$^+$ = 2923.53) (mass spectrum for PF-750 not shown). DMSO-treated controls exclusively showed mass signals for the unmodified Ser241-containing tryptic peptide (calculated MH$^+$ = 2670.33, observed MH$^+$ = 2670.43) (Figure 5A). No signal was detected for the C(O)−NHPh modification of FAAH in either PF-750- and PF-622-treated samples. These data indicate that the binding orientation of the urea inhibitors places the aniline moiety in the cytoplasmic access channel and the piperazine/piperidine portion of the molecule in the acyl chain binding channel of the FAAH active site. Thus, the aniline group serves as the leaving groups similar to the ethanolamine moiety of anandamide or the aryloxy substituents of URB-597 and related carbamate inhibitors (*27*).

Selectivity of FAAH Inhibitors in Human and Mouse Proteomes. To assess the selectivity of the piperidine/piperazine urea series, PF-750 was profiled by competitive ABPP at 500 μM in a number of different proteomes derived from mouse and human sources. Competitive ABPP involves the coordinated application of a candidate inhibitor and a reporter-tagged fluorophosphonate (FP) probe (*25*), which serves as a general activity-based profiling tool for the serine hydrolase superfamily (*29, 41*). Serine hydrolases that show significant reductions in probe labeling intensity in the presence of inhibitor are scored as targets of the compound. In this way, competitive ABPP provides a global view of the proteome-wide selectivity of serine hydrolase inhibitors. The selectivity of PF-750 was compared to those of several other FAAH inhibitors including URB-597, OL-135, and CAY-10402, which were profiled at 100 μM. Representative gel images of soluble proteomes of mouse liver, human liver, and human testis are shown in Figure 6. Consistent with previous reports of multiple serine hydrolase targets for URB-597, OL-135, and CAY-10402 (*25, 26, 28*), we also observed multiple off targets for these inhibitors, particularly among FP-labeled proteins migrating between 55 and 65 kDa. In contrast, no off targets were observed for PF-750 tested at 500 μM. Importantly, under these conditions, all four
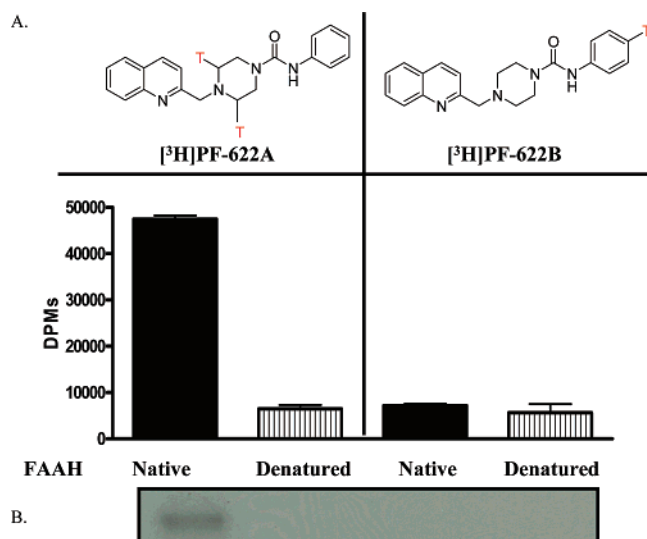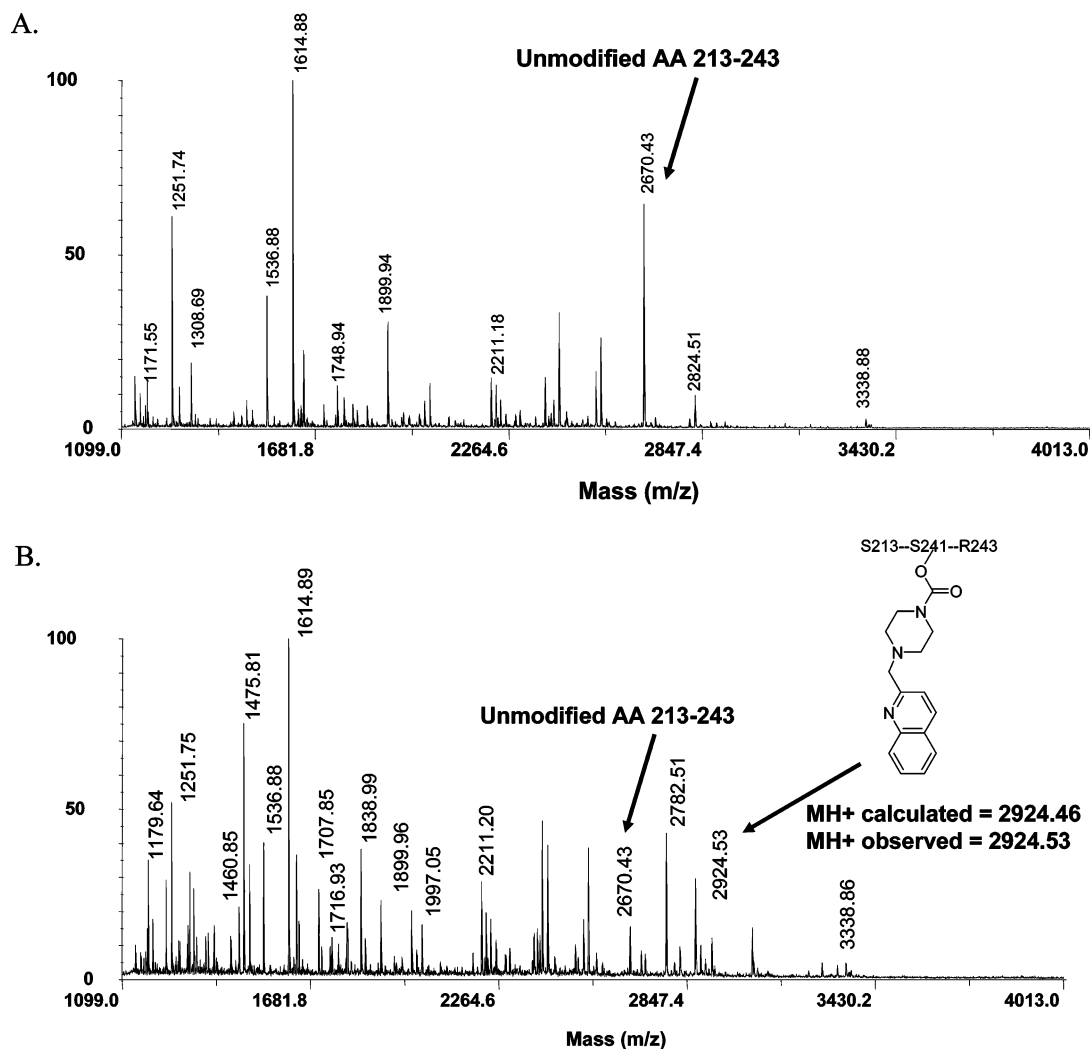
FIGURE 5: PF-622 inhibits hFAAH by carbamylation of the active site amino acid residue Ser241 nucleophile. The MS data supports pathway A in Scheme 2. MALDI-MS mapping of a tryptic digest of purified hFAAH pretreated with (A) DMSO and (B) PF-622. A new tryptic peptide with mass that corresponds to the amino acid 213−243 peptide that is modified by the CO-piperazinyl moiety of PF-622 is highlighted.

inhibitors completely inhibited FAAH from both mouse and human brain membranes (Figure 6D).

To verify that potential serine hydrolase targets of PF-750 were not missed by gel analysis due to either low abundance or comigrating proteins, mouse liver soluble proteome was subjected to a competitive ABPP reaction between a rhodamine-tagged FP probe and each of the aforementioned FAAH inhibitors (PF-750 at 500 μM; all others at 100 μM) or DMSO, captured with rhodamine antibodies, and identified by MS analysis as described in the Materials and Methods section. The parent ion intensities of FP-labeled active site tryptic peptides for 21 serine hydrolases were comparatively quantified in inhibitor- and DMSO-treated samples. The resulting target selectivity profiles are shown in Figure 7. A number of hydrolase targets were observed for URB-597, OL-135, and CAY-10402 including carboxyesterase 1, 3, 22, and AU018778 as well as multiple hydrolases not previously reported as targets of FAAH inhibitors (acyl protein thioesterase, arylacetamide deacetylase, and platelet activating factor (PAF) acetylhydrolase). In contrast, none of the serine hydrolases in soluble mouse liver proteome were inhibited by PF-750 (note that FAAH, which is an integral membrane protein, is not present

in this proteomic fraction). These higher resolution LC-MS data thus provide further evidence that PF-750 is a highly selective FAAH inhibitor.

Previous studies have shown that OL-135 is quite selective for FAAH at lower concentrations (e.g., <10 μM; 26). To determine the selectivity of URB-597 and CAY-10402 at lower concentrations, these inhibitors were titrated in competitive ABPP assays using the soluble mouse liver proteome. The resulting inhibition profiles for individual serine hydrolases at different concentrations of CAY-10402 and URB-597 are shown together with their approximate IC$_{50}$ values in Figure 7. One of the most strongly inhibited enzymes for all three reference inhibitors was carboxylesterase 3 (triacylglycerol hydrolase) (marked with an arrow in Figure 7), a well-known off target for FAAH inhibitors (25, 26).

Although carboxylesterases have already been reported as off targets for URB-597 (25−28), the potency of this inhibitor for individual carboxylesterases has not been well characterized in native liver proteomes due to the presence of many members of this enzyme class that comigrate by 1D SDS-PAGE. In principle, quantifying serine hydrolases by the mass spectrometric method described herein should provide enhanced resolution of these targets and allow
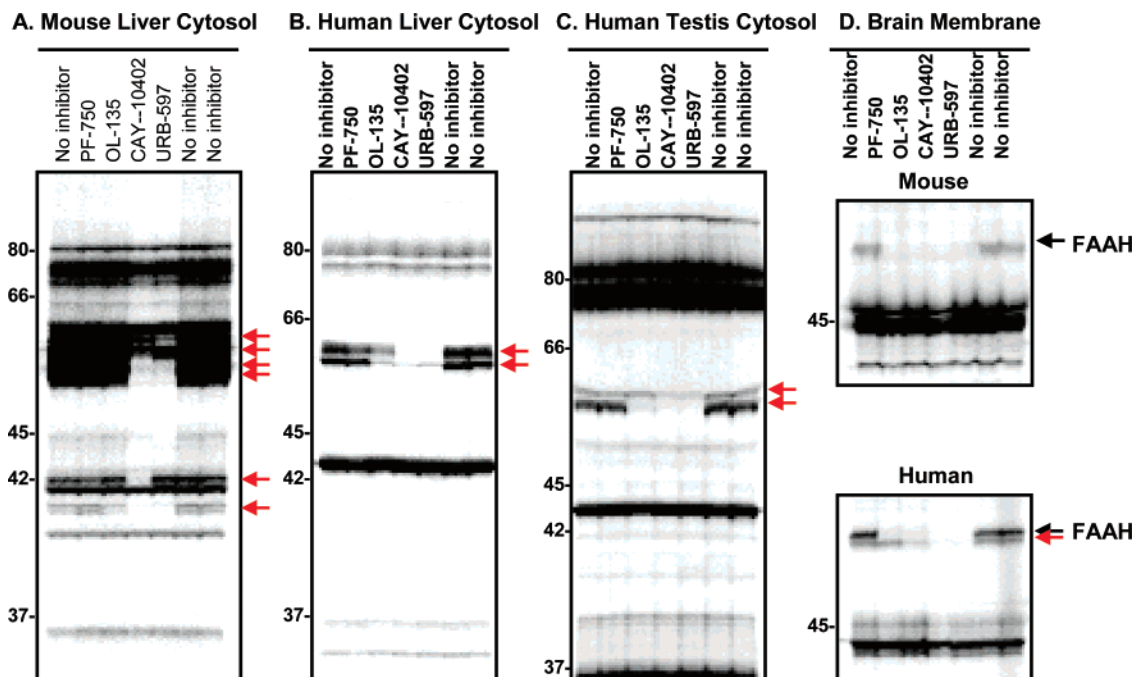
FIGURE 6: Selectivity profiling of FAAH inhibitors in human and mouse proteomes. Gel images of proteomes labeled with FP-Rh after incubating with either inhibitors (PF-750 at 500 μM; OL-135, CAY-10402, and URB-597 at 100 μM) or DMSO for 1 h at RT followed by overnight incubation at 4 °C. Inhibited bands are shown with red arrows: (A) soluble mouse liver proteome, (B) soluble human liver proteome, (C) soluble human testis proteome, (D, upper panel) mouse brain membrane proteome, and (D, lower panel) human brain membrane proteome.

Color legend:
- >90% Inhibition
- 70 - 89% Inhibition
- 50 - 69% Inhibition
- 30 - 49% Inhibition
- No Inhibition

Reference	Annotation	PF-750 (500)	OL-135 (100)	CAY-10402 IC50 (μM)	URB-597 IC50 (μM)	Mouse IC50 (μM)	Rat IC50 (μM)
UniRef100_P97823	Acyl-protein thioesterase 1						
UniRef100_Q99PG0	Arylacetamide deacetylase			4.5			
UniRef100_Q8R097	Carboxylestease 2210023G05Rik				30		
UniRef100_Q8VCC2	Carboxylesterase 1			0.22	50		
UniRef100_Q64176	Carboxylesterase 22			<0.2	3.9		7.36[c]
UniRef100_Q8VCT4	Carboxylesterase 3			<0.2	0.49	0.192[a]	
UniRef100_Q63880	Carboxylesterase 31				>50	>100[b]	
UniRef100_Q8BK48	Carboxylesterase 5			<0.2	0.26		
UniRef100_Q8QZR3	Carboxylesterase 6				0.62	0.2[b]	1.62[c]
UniRef100_Q91WU0	Carboxylesterase AU018778			<0.2	0.33		0.21[c]
UniRef100_P23953	Carboxylesterase N				>50		>100[c]
UniRef100_Q03311	Cholinesterase precursor				8.5		
UniRef100_Q8VCU1	Esterase 31-like						
UniRef100_Q8VDG7	PAF acetylhydrolase 2						
UniRef100_Q8R146	Acylamino-acid-releasing enzyme						
UniRef100_P28843	Dipeptidyl peptidase 4						
UniRef100_P05208	Elastase-2						
UniRef100_Q9R0P3	Esterase D						
UniRef100_P27656	Hepatic triacylglycerol lipase						
UniRef100_Q9DB29	Lipolytic enzyme GDSL						
UniRef100_O35448	Palmitoyl-protein thioesterase 2						

Concentration (μM): PF-750 = 500; OL-135 = 100; CAY-10402 = 100, 50, 5, 0.5; URB-597 = 100, 50, 5, 0.5. Published IC50 values for URB-597 off-targets given for Mouse and Rat.

[a]Ref 26: [b]Ref 27: [c]Ref 28.

FIGURE 7: Selectivity profiling of FAAH inhibitors in mouse soluble liver proteome as determined by mass spectrometry. Soluble liver proteomic samples either in the absence or presence of inhibitor at the indicated concentrations were prepared for mass spectrometry as described in Materials and Methods. The serine hydrolase peptides were quantified by mass spectrometry, and the percentage inhibition at different inhibitor concentrations are shown. Where applicable, the approximate IC$_{50}$ values are included.

estimation of IC$_{50}$ values. To address this possibility, CAY-10402 and URB-597 were titrated into soluble mouse liver proteome (50, 5, and 0.5 μM), and following competitive ABPP reactions, the serine hydrolase signals were quantified by mass spectrometry. For each off target, the percentage inhibition was plotted versus the inhibitor concentration to calculate IC$_{50}$ values. Among the inhibitors used in this study, URB-597 has been the most extensively characterized in terms of its interactions with the serine hydrolase proteome with several reported IC$_{50}$ values in the literature (26−28).
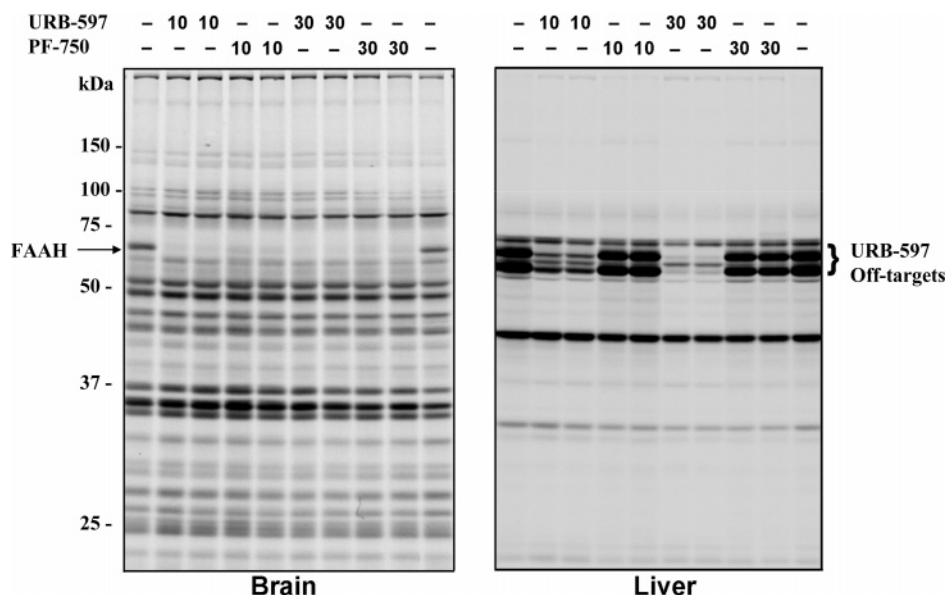
FIGURE 8: Profiling the in vivo selectivity of FAAH inhibitors by competitive ABPP. Mice were treated with PF-750 or URB-597 at the indicated doses (i.p.) for 1 h and then sacrificed and tissue removed for competitive ABPP analysis with FP-rhodamine. Serine hydrolase targets of PF-750 and URB-597 were detected by SDS-PAGE and in-gel fluorescence scanning. Note that both PF-750 and URB-597 are highly selective for FAAH in mouse brain membrane proteomes, but the latter inhibitor targets several additional serine hydrolases in mouse liver membrane proteome.

These values are shown in Figure 7 with the corresponding values for the off targets determined in this study. Overall, the IC_{50} values obtained in this study were consistent with the published values, thus validating this mass spectrometric approach toward determining IC_{50} values in native proteomes.

Profiling the Selectivity of FAAH Inhibitors in Vivo. To confirm that the different selectivity profiles of FAAH inhibitors determined in vitro were also observed in vivo, we treated wild-type mice with vehicle, PF-750 (10 or 30 mg/kg, i.p.), or URB-597 (10 or 30 mg/kg, i.p.) for 1 h, after which the animals were sacrificed and their tissues harvested and profiled for changes in serine hydrolase activity using FP-Rh. At each dose tested, both URB-597 and PF-750 selectively targeted FAAH in the brain (Figure 8). PF-750 showed no detectable off-target activity in peripheral tissues (e.g., liver; Figure 8). In contrast, URB-597 was found to block FP labeling of several liver serine hydrolases between the molecular masses of 55 and 65 kDa (Figure 8). The extent of blockade was dose dependent, with a nearly complete inhibition of probe labeling being observed at the 30 mg/kg dose of URB-597. In previous studies we have shown that these major liver targets of URB-597 do not correspond to FAAH but rather represent members of the carboxylesterase family of serine hydrolases (*27*). These data indicate that both URB-597 and PF-750 selectively inactivate FAAH in the CNS, but only the latter compound does so without also perturbing enzyme activities in peripheral tissues.

DISCUSSION

In this report, we described a novel mechanistic class of FAAH inhibitors embodied by PF-750 and PF-622. These inhibitors operate by a covalent, irreversible mechanism, utilizing a piperidine/piperazine urea group as a tempered electrophile that carbamylates FAAH's catalytic Ser241 nucleophile. The time-dependent inhibition by PF-750 and PF-622 combined with results showing no activity recovery in the rapid dilution studies indicated that their mechanism

of inhibition is either slowly reversible time-dependent inhibition or covalent irreversible inhibition (Scheme 1). We then verified formation of covalent modification by two different methods. First we demonstrated the covalent labeling of FAAH by incorporation of [^{3}H]PF-622 into the enzyme. To differentiate between the two possible carbamylation reactions with the enzyme's Ser241 nucleophile, we introduced tritium on either side of the urea bond of the inhibitor, which demonstrated that the aniline portion of the urea served as the leaving group. Second, we determined by MALDI-MS analysis that the piperidine/piperazine moiety of PF-750 and PF-622 is covalently attached to Ser241 in the FAAH active site. These data indicate that the binding orientation of the urea inhibitors may place the aniline and piperazine/piperidine moieties in the cytoplasmic access and acyl chain-binding channel of FAAH (*42*), respectively. This type of information could be potentially used to further enhance potencies of this chemical series as shown for the carbamates (*27*). Elucidation of the irreversible mode of action of the piperidine/piperazine ureas has prompted us to modify the FAAH assay so that inhibitor potencies could be measured as k_{inact}/K_i values, the details of which will be discussed in a future publication. Unlike IC_{50} values, k_{inact}/K_i values do not change with various preincubation times and have been described as the best measure of potencies for irreversible inhibitors (*43*).

Almost 30% of the marketed drugs whose molecular targets are enzymes act by irreversible inhibition (*44*). This high percentage is rather surprising considering the strong bias against developing irreversible inhibitors as clinical candidates in the pharmaceutical industry. One of the main rationales for this bias is derived from the high inherent reactivity of functional groups generally associated with covalent modifications of proteins. Excessively reactive covalent modifiers can form covalent bonds with a large number of enzymes/proteins, often within the same mechanistic class (*45*). Compounding these concerns, there has

Scheme 3
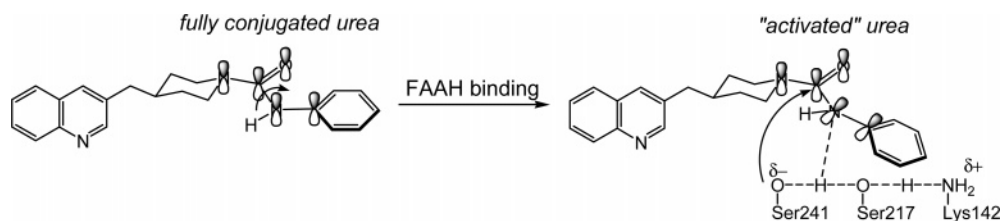
historically been no direct way to evaluate the selectivity of covalent inhibitors against a large number of enzymes in the same class. Traditional approaches for testing selectivity have involved setting up individual substrate-based assays with a limited number of candidate "off target" enzymes. However, this approach excludes the analysis of uncharacterized enzymes due to the lack of substrate-based assays. More recently, functional proteomic methods, such as competitive ABPP, have emerged that enable selectivity of inhibitors to be evaluated against numerous enzymes in parallel directly in native cells and tissues (*25*, *46*).

In order to extensively assess the selectivity of PF-750, we utilized competitive ABPP to evaluate the targets of this inhibitor in multiple human and mouse tissue proteomes. These studies were conducted with other classes of FAAH inhibitors that have been shown to exhibit variable degrees of selectivity. Our data revealed that the piperidine/piperazine ureas are highly selective FAAH inhibitors, showing no discernible activity against other serine hydrolases in vitro or in vivo at concentrations up to 500 μM and 30 mg/kg (i.p.), respectively. These results contrasted sharply with the properties of other classes of FAAH inhibitors, including URB-597, OL-135, and CAY-10402, which all targeted multiple serine hydrolases in addition to FAAH in human and mouse proteomes.

It is worth speculating on the origin of the remarkable selectivity displayed by the piperidine/piperazine ureas for FAAH relative to other members of the serine hydrolase superfamily. Given the inherent chemical stability of the urea bond, it was rather unexpected to find that PF-750 and PF-622 inhibit FAAH by covalent modification. Indeed, in contrast to carbamates, ureas require exposure to extreme conditions such as strong acid/base with overnight reflux to promote chemical hydrolysis. It is thus likely that the specificity observed for piperidine/piperizine urea inhibitors is at least partly due to their chemical stability, which might make these agents uniquely susceptible to reaction with FAAH, which is an amidase, and inert to the vast majority of other serine hydrolases, which primarily accept esters/ thioesters as substrates. Literature searches yielded no other examples of piperidine/piperzine ureas as irreversible inhibitors of serine hydrolases, further underscoring the potential novelty of the urea functional group as a mode for covalent modification of an enzyme from this class. Interestingly, additional reports of urea-based inhibitors of FAAH have recently appeared in the patent literature (*30*, *47*). The mechanism of inhibition for these agents remains unexamined, but our results would argue that they likely also act by a covalent, irreversible mechanism.

FAAH has been shown to hydrolyze amides and esters at equivalent rates, which distinguishes this enzyme from most other serine hydrolases that prefer the latter class of substrates (*48*). This unusual feature appears to be due, at least in part,

to the serine–serine–lysine catalytic triad in the FAAH active site, with the catalytic lysine (Lys142) functioning as both a base involved in the activation of the Ser241 nucleophile and an acid that participates in the protonation of the substrate leaving group (*49*) (Scheme 3). Therefore, nucleophilic attack and leaving-group protonation occur in a coordinated manner. This in part explains why amides are good substrates for FAAH, but it cannot completely rationalize why the ureas described in this manuscript are able to act as "suicide substrates" or irreversible inhibitors. An additional activation step must take place upon binding in the FAAH active site, which renders the reactivity of the urea similar to that of an amide. We hypothesize that catalysis of the acylation reaction could also be partially derived from a binding-induced conformational change in the piperidine/ piperazine urea that diminishes conjugation of the nitrogen lone pair with the carbonyl, which activates the urea toward nucleophile attack (*50*) as shown in Scheme 3. If this binding-induced activation of the urea is FAAH specific, it could also help explain the remarkable selectivity of these ureas as inhibitors for this enzyme.

ACKNOWLEDGMENT

REFERENCES

1. Cravatt, B. F., Giang, D. K., Mayfield, S. P., Boger, D. L., Lerner, R. A., and Gilula, N. B. (1996) Molecular characterization of an enzyme that degrades neuromodulatory fatty-acid amides, *Nature 384*, 83–87.

2. Giang, D. K., and Cravatt, B. F. (1997) Molecular characterization of human and mouse fatty acid amide hydrolases, *Proc. Natl. Acad. Sci. U.S.A. 94*, 2238–2242.

3. Devane, W. A., Hanus, L., Breuer, A., Pertwee, R. G., Stevenson, L. A., Griffin, G., Gibson, D., Mandelbaum, A., Etinger, A., and Mechoulam, R. (1992) Isolation and structure of a brain constituent that binds to the cannabinoid receptor, *Science 258*, 1946–1949.

4. Lambert, D. M., Vandevoorde, S., Jonsson, K. O., and Fowler, C. J. (2002) The palmitoylethanolamide family: a new class of anti-inflammatory agents?, *Curr. Med. Chem. 9*, 663–674.

5. Cravatt, B. F., Prospero-Garcia, O., Siuzdak, G., Gilula, N. B., Henriksen, S. J., Boger, D. L., and Lerner, R. A. (1995) Chemical characterization of a family of brain lipids that induce sleep, *Science 268*, 1506–1509.

6. Rodriguez de Fonseca, F., Navarro, M., Gomez, R., Escuredo, L., Nava, F., Fu, J., Murillo-Rodriguez, E., Giuffrida, A., LoVerme, J., Gaetani, S., Kathuria, S., Gall, C., and Piomelli, D. (2001) An anorexic lipid mediator regulated by feeding, *Nature 414*, 209–212.

7. Cravatt, B. F., Demarest, K., Patricelli, M. P., Bracey, M. H., Giang, D. K., Martin, B. R., and Lichtman, A. H. (2001) Supersensitivity to anandamide and enhanced endogenous cannabinoid signaling in mice lacking fatty acid amide hydrolase, *Proc. Natl. Acad. Sci. U.S.A. 98*, 9371−9376.

8. Kathuria, S., Gaetani, S., Fegley, D., Valino, F., Duranti, A., Tontini, A., Mor, M., Tarzia, G., La Rana, G., Calignano, A., Giustino, A., Tattoli, M., Palmery, M., Cuomo, V., and Piomelli, D. (2003) Modulation of anxiety through blockade of anandamide hydrolysis, *Nat. Med. 9*, 76−81.

9. Lichtman, A. H., Shelton, C. C., Advani, T., and Cravatt, B. F. (2004) Mice lacking fatty acid amide hydrolase exhibit a cannabinoid receptor-mediated phenotypic hypoalgesia, *Pain 109*, 319−327.

10. Hohmann, A. G., Suplita, R. L., Bolton, N. M., Neely, M. H., Fegley, D., Mangieri, R., Krey, J. F., Walker, J. M., Holmes, P. V., Crystal, J. D., Duranti, A., Tontini, A., Mor, M., Tarzia, G., and Piomelli, D. (2005) An endocannabinoid mechanism for stress-induced analgesia, *Nature 435*, 1108−1112.

11. Chang, L., Luo, L., Palmer, J. A., Sutton, S., Wilson, S. J., Barbier, A. J., Breitenbucher, J. G., Chaplan, S. R., and Webb, M. (2006) Inhibition of fatty acid amide hydrolase produces analgesia by multiple mechanisms, *Br. J. Pharmacol. 148*, 102−113.

12. Jayamanne, A., Greenwood, R., Mitchell, V. A., Aslan, S., Piomelli, D., and Vaughan, C. W. (2006) Actions of the FAAH inhibitor URB597 in neuropathic and inflammatory chronic pain models, *Br. J. Pharmacol. 147*, 281−288.

13. Russo, R., LoVerme, J., La Rana, G., Compton, T., Parrot, J., Duranti, A., Tontini, A., Mor, M., Tarzia, G., Calignano, A., and Piomelli, D. (2007) The fatty-acid amide hydrolase inhibitor URB597 (cyclohexyl carbamic acid 3′-carbamoyl-biphenyl-3-yl ester) reduces neuropathic pain after oral administration in mice, *J. Pharmacol. Exp. Ther. 322*, 236−242.

14. Gobbi, G., Bambico, F. R., Mangieri, R., Bortolato, M., Campolongo, P., Solinas, M., Cassano, T., Morgese, M. G., Debonnel, G., Duranti, A., Tontini, A., Tarzia, G., Mor, M., Trezza, V., Goldberg, S. R., Cuomo, V., and Piomelli, D. (2005) Antidepressant-like activity and modulation of brain monoaminergic transmission by blockade of anandamide hydrolysis, *Proc. Natl. Acad. Sci. U.S.A. 102*, 18620−18625.

15. Naiu, P. S., Varvel, S. A., Ahn, K., Cravatt, B. F., Martin, B. R., and Lichtman, A. H. (2006) Evaluation of fatty acid amide hydrolase inhibition in murine models of emotionality, *Psychopharmacology 192*, 61−70.

16. Huitron-Resendiz, S., Sanchez-Alavez, M., Wills, D. N., Cravatt, B. F., and Henriksen, S. J. (2004) Characterization of the sleep-wake patterns in mice lacking fatty acid amide hydrolase, *Sleep 27*, 857−865.

17. Cravatt, B. F., Saghatelian, A., Hawkins, E. G., Clement, A. B., Bracey, M. H., and Lichtman, A. H. (2004) Functional disassociation of the central and peripheral fatty acid amide signaling systems, *Proc. Natl. Acad. Sci. U.S.A. 101*, 10821−10826.

18. Holt, S., Comelli, F., Costa, B., and Fowler, C. J. (2005) Inhibitors of fatty acid amide hydrolase reduce carrageenan-induced hind paw inflammation in pentobarbital-treated mice: comparison with indomethacin and possible involvement of cannabinoid receptors, *Br. J. Pharmacol. 146*, 467−476.

19. Chebrou, H., Bigey, F., Arnaud, A., and Galzy, P. (1996) Study of the amidase signature group, *Biochim. Biophys. Acta 1298*, 285−293.

20. McKinney, M. K., and Cravatt, B. F. (2005) Structure and function of fatty acid amide hydrolase, *Annu. Rev. Biochem. 74*, 411−432.

21. Patricelli, M. P., Lovato, M. A., and Cravatt, B. F. (1999) Chemical and mutagenic investigations of fatty acid amide hydrolase: evidence for a family of serine hydrolases with distinct catalytic properties, *Biochemistry 38*, 9804−9812.

22. Patterson, J. E., Ollman, I. R., Cravatt, B. F., Boger, D. L., Wong, C. H., and Lerner, R. A. (1996) Inhibition of oleamide hydrolase catalyzed hydrolysis of the endogenous sleep-inducing lipid *cis*-9-octadecenamide, *J. Am. Chem. Soc. 118*, 5938−5945.

23. Romero, A., Du, W., Hwang, I., Rayl, T. J., F. Kimball, S., Leung, D., Hoover, H. S., Apodaca, R. L., Breitenbucher, J. G., Cravatt, B. F., and Boger, D. L. (2007) Potent and selective alpha-ketoheterocycle-based inhibitors of the anandamide and oleamide

24. catabolizing enzyme, fatty acid amide hydrolase, *J. Med. Chem. 50*, 1058−1068.

24. Boger, D. L., Miyauchi, H., Du, W., Hardouin, C., Fecik, R. A., Cheng, H., Hwang, I., Hedrick, M. P., Leung, D., Acevedo, O., Guimaraes, C. R. W., Jorgensen, W. L., and Cravatt, B. F. (2005) Discovery of a potent, selective, and efficacious class of reversible α-ketoheterocycle inhibitors of fatty acid amide hydrolase effective as analgesics, *J. Med. Chem. 48*, 1849−1856.

25. Leung, D., Hardouin, C., Boger, D. L., and Cravatt, B. F. (2003) Discovering potent and selective reversible inhibitors of enzymes in complex proteomes, *Nat. Biotechnol. 21*, 687−691.

26. Lichtman, A. H., Leung, D., Shelton, C. C., Saghatelian, A., Hardouin, C., Boger, D. L., and Cravatt, B. F. (2004) Reversible inhibitors of fatty acid amide hydrolase that promote analgesia: evidence for an unprecedented combination of potency and selectivity, *J. Pharmacol. Exp. Ther. 311*, 441−448.

27. Alexander, J. P., and Cravatt, B. F. (2005) Mechanism of carbamate inactivation of FAAH: Implications for the design of covalent inhibitors and in vivo functional probes for enzymes, *Chem. Biol. 12*, 1179−87.

28. Zhang, D., Saraf, A., Kolasa, T., Bhatia, P., Zheng, G. Z., Patel, M., Lannoye, G. S., Richardson, P., Stewart, A., Rogers, J. C., Brioni, J. D., and Surowy, C. S. (2007) Fatty acid amide hydrolase inhibitors display broad selectivity and inhibit multiple carboxylesterases as off-targets, *Neuropharmacology 52*, 1095−1105.

29. Patricelli, M. P., Giang, D. K., Stamp, L. M., and Burbaum, J. J. (2001) Direct visualization of serine hydrolase activities in complex proteome using fluorescent active site-directed probes, *Proteomics 1*, 1067−1071.

30. Apodaca, R., Breitenbucher, J. G., Pattabiraman, K., Seierstad, M., and Xiao, W. (2006) Piperazinyl and piperidinyl ureas as modulators of fatty acid amide hydrolase, *WO 2006/074025*.

31. Patricelli, M. P., Lashuel, H. A., Giang, D. K., Kelly, J. W., and Cravatt, B. F. (1998) Comparative characterization of a wild type and transmembrane domain-deleted fatty acid amide hydrolase: identification of the transmembrane domain as a site for oligomerization, *Biochemistry 37*, 15177−87.

32. Ahn, K. (2006) Fatty acid amide hydrolase assay, *WO 2006/085196*.

33. De Bank, P. A., Kendall, D. A., and Alexander, S. P. (2005) A spectrophotometric assay for fatty acid amide hydrolase suitable for high-throughput screening, *Biochem. Pharmacol. 69*, 1187−93.

34. Shevchenko, A., Wilm, M., Vorm, O., and Mann, M. (1996) Mass spectrometric sequencing of proteins from silver-stained polyacrylamide gels, *Anal. Chem. 68*, 850−8.

35. Perkins, D. N., Pappin, D. J. C., Creasy, D. M., and Cottrell, J. S. (1999) Probability-based protein identification by searching sequence databases using mass spectrometry data, *Electrophoresis 20*, 3551−67.

36. Nomanbhoy, T. K., Rosenblum, J., Aban, A., and Burbaum, J. J. (2003) Inhibitor focusing: direct selection of drug targets from proteomes using activity-based probes, *Assay Drug Dev. Technol. 1*, 137−146.

37. Jessani, N., Liu, Y., Humphrey, M., and Cravatt, B. F. (2002) Enzyme activity profiles of the secreted and membrane proteome that depict cancer cell invasiveness, *Proc. Natl. Acad. Sci. U.S.A. 99*, 10335−10340.

38. Okerberg, E. S., Wu, J., Zhang, B., Samii, B., Blackford, K., Winn, D. T., Shreder, K. R., Burbaum, J. J., and Patricelli, M. P. (2005) High-resolution functional proteomics by active-site peptide profiling, *Proc. Natl. Acad. Sci. U.S.A. 102*, 4996−5001.

39. Patricelli, M. P., Szardenings, A. K., Liyanage, M., Nomanbhoy, T. K., Wu, M., Weissig, H., Aban, A., Chun, D., Tanner, S., and Kozarich, J. W. (2007) Functional interrogation of the kinome using nucleotide acyl phosphates, *Biochemistry 46*, 350−358.

40. Yates, J. R., III, Eng, J. K., McCormack, A. L., and Schieltz, D. (1995) Method to correlate tandem mass spectra of modified peptides to amino acid sequences in the protein database, *Anal. Chem. 67*, 1426−1436.

41. Liu, Y., Patricelli, M. P., and Cravatt, B. F. (1999) Activity-based protein profiling: the serine hydrolases, *Proc. Natl. Acad. Sci. U.S.A. 96*, 14694−14699.

42. Bracey, M. A., Hanson, M. A., Masuda, K. R., Stevens, R. C., and Cravatt, B. F. (2002) Structural adaptation in a membrane enzyme that terminates endocannabinoid signaling, *Science 298*, 1793−1796.

43. Copeland, R. A. (2000) *Enzymes: A practical introduction to structure, mechanism, and data analysis*, 2nd ed., pp 318−349, Wiley-VCH Press, New York.

44. Robertson, J. G. (2005) Mechanistic basis of enzyme-targeted drugs, *Biochemistry 44*, 5561−5571.

45. Alexander, J. P., and Cravatt, B. F. (2006) The putative endocannabinoid transport blocker LY2183240 is a potent inhibitor of FAAH and several other brain serine hydrolases, *J. Am. Chem. Soc. 128*, 9699 -9704.

46. Greenbaum, D., Baruch, A., Hayrapetian, L., Darula, Z., Burlingame, A., Medzihradszky, K. F., and Bogyo, M. (2002) Chemical approaches for functionally probing the proteome, *Mol. Cell. Proteomics 1*, 60−68.

47. Matsumoto, T., Kori, M., Miyazaki, J., and Kiyota, Y. (2006) Preparation of piperidinecarboxamides and piperazinecarboxam-ides as fatty acid amide hydrolase (FAAH) inhibitors, *WO 2006/054652*.

48. Patricelli, M. P., and Cravatt, B. F. (1999) Fatty acid amide hydrolase competitively degrades bioactive amides and esters through a nonconventional catalytic mechanism, *Biochemistry 38*, 14125−14130.

49. McKinney, M. K., and Cravatt, B. F. (2003) Evidence for the distinct roles in catalysis for residues of the serine-serine-lysine catalytic triad of fatty acid amide hydrolase, *J. Biol. Chem. 278*, 37393−37399.

50. Boger, D. L., and Garbaccio, R. M. (1997) Catalysis of the CC-1065 and duocarmycin DNA alkylation reaction: DNA binding induced conformational change in the agent results in activation, *Bioorg. Med. Chem. 5*, 263−276.

BI701378G